Mechanistic Understanding of the Effect of Temperature and Salinity on the Water/Toluene Interfacial Tension

Cuiying Jian[†,‡], *Mohammad Reza Poopari*[‡], *Qingxia Liu*[‡], *Nestor Zerpa*[§],

Hongbo Zeng[‡,*], *and Tian Tang*[†,*]

[†] Department of Mechanical Engineering and

[‡] Department of Chemical and Material Engineering,

University of Alberta, Edmonton, and

[§]Nexen Energy ULC, A CNOOC Limited Company, Calgary

AB, Canada

[*]Corresponding authors;

Phone: +1-780-492-1044. Fax: +1-780-492-2881. E-mail: hongbo.zeng@ualberta.ca (H.Z.)

Phone: +1-780-492-5467. Fax: +1-780-492-2200. E-mail: tian.tang@ualberta.ca (T.T.)

Abstract: In this work, a series of pendant drop measurements and molecular dynamics (MD) simulations were performed to investigate the effects of temperature and salinity on the interfacial tension (IFT) of water/toluene binary systems. Both experimental measurements and theoretical simulations demonstrated that elevating temperature decreased the IFT while adding salts resulted in an increment of IFT. Furthermore, it was found that the presence of model asphaltene compound could alleviate the effects of temperature and salinity on the IFTs. That is, in the presence of the model asphaltene compound, the decrement effect of elevating temperature as well as the increment effect of adding salts was reduced. Through detailed analysis of the simulated systems, the underlying mechanisms for the effects of temperature and salinity on the IFTs were clarified for cases with and without the presence of the model asphaltene. The results reported here can help to modulate the IFT values of oil/water interfaces in petroleum processing.

1. INTRODUCTION

Interfacial tension (IFT), as a fundamental thermodynamic quantity, can be experimentally measured and has strong influences on the dynamics and morphologies of multiphase systems. [1-4] In the particular area of petroleum processing, a large amount of oil/water (O/W) interfaces are generated due to the wide usage of water.[5] Proper modulation of the IFT of O/W systems can facilitate the heavy oil extraction and transportation processes. For these purposes, great efforts have been dedicated to gaining detailed knowledge on the IFT of O/W systems.[6-20]

Petroleum processing usually employs a wide range of temperature, pressure, and water salinity.[6-9] Hence a series of experimental measurements were performed to investigate these physical (or/and chemical) conditions on the IFTs of water/organic-solvent interfaces.[6-11] Generally, it was concluded that increasing temperature reduced the IFT while adopting higher pressure or adding inorganic salts into aqueous phase increased the IFT.[6-11] Following these first efforts, experimental measurements were then further performed on the IFTs of crude/oil-water interfaces. Moeini et al.[12] performed IFT measurements on an Iranian crude oil/water interface using pendant drop technique under a wide range of temperature, pressure, and salt concentrations. It was reported[12] that increasing temperature decreased the IFT while elevating pressure slightly increased the IFT, similar to that observed for the IFTs of water/organic-solvent interfaces[6-11]. On the other hand, chlorate concentrations showed a non-monotonic effect on the IFT in which the IFT value of crude oil/water interface was minimized at a critical salt concentration.[12] In contrast, Lashkarbolookia et al.[13] showed that the effect of salinity depends on the ion species. In their work,[13] while sulfate had a non-monotonic effect on the IFTs, chlorate decreased the IFT values of crude oil/water interface.

Besides these controlled conditions, the presence of interfacial-active oil components, such as asphaltenes, decreases the water/oil IFT. The so-induced IFT reduction can be correlated with the stability of water-in-oil emulsions and have important implications on understanding the interfacial properties of asphaltenes.[14-17] Therefore, the effect of asphaltenes on the IFTs under various conditions has also been extensively discussed in the literature. For instance, Banerjee and co-workers[15-17] performed pendant drop measurements on the water/organic solvent (mixtures of aliphatic base oil and toluene) IFT under different asphaltene concentrations and solvent viscosities. Their results revealed that the IFT of organic solvents/water interface monotonically decreased with increasing surface coverage of asphaltenes. Furthermore, in the presence of salt, Lashkarbolookia et al.[18] suggested the existence of a critical $MgCl_2$ and $CaCl_2$ concentration, where the minimum IFT of asphaltene-toluene solution/water interface was reported. In contrast, sodium carbonate was reported to decrease the IFT of asphaltene-model oil/water interface in the work of Guo et al.[19] In addition, the effect of pH on the water/oil IFTs as well as the synergetic effects of asphaltenes and other oil components (e.g. maltenes and naphthenic acids) has also been discussed in literature.[14, 20]

Despite the significant amount of existing experimental work, mechanistic understanding of the O/W IFT is still far from being complete. Direct explanations from the atomic perspective on the observed effect of external conditions, especially in the presence of asphaltenes, are not available in the literature. While molecular dynamics (MD) techniques have been implemented extensively before to study petroleum systems,[21-34] its application to evaluate IFT of oil/water interface in the presence of asphaltenes has been challenged with the significantly different asphaltene concentrations used in experiments and simulations. Due to the limited system size that can be simulated, the asphaltene concentration in simulations is usually much larger than that in experiments. Only in our very recent work[35] was this issue clarified, where the surface concentration, instead of bulk concentration, of asphaltenes was found to govern the reduction of IFT. That is, the much higher bulk concentration in simulations actually leads to a surface concentration similar to that in experiments, and thus can result in an IFT reduction that is comparable to experimental observations.

Motivated by these efforts, the objective of our current work is to present a mechanistic understanding, from atomic level, of the effects of temperature and salinity on IFT in the presence and absence of asphaltenes at the O/W interfaces. The information from this study will not only benefit the study of O/W interface in petroleum processing, but also shed lights on many other industrial applications where interfaces containing liquid phases are employed. For instance, gas/liquid, vapour/liquid, and solid/liquid interfaces are commonly employed in a wide range of industrial applications, such as the processing of functional materials, ink-jet printing, and coating flow technology.[36-38] The remainder of this article is organized as following: section 2 introduces the systems studied; in section 3, our MD results were first validated through comparison with pendant drop measurements, followed by a detailed analysis of the underlying mechanism of the effect of different conditions on the IFTs; and final conclusion is given in section 4.

2. METHODS

In this work, the oil phase was represented by toluene, considering the natural occurrence of toluene in crude oil as well as its wide usage in separating asphaltenes from fine solids.[39,40]

Violanthrone-79 (VO-79) was chosen as a representative model for asphaltene molecules, and its chemical structure is shown in Figure 1. The detailed rationale for selecting this particular model was described in our previous work.[35] Briefly, VO-79 shares certain structural similarities with the island-type structure proposed for asphaltene molecules in the literature,[41] and its oxygen content (9.0%) is close to that of the asphaltene fractions stabilizing O/W emulsions (5.54%).[42] However, it should be noted that, despite the previous work,[35] it remains to be further investigated whether the intermolecular interactions of VO-79 and surrounding water and/or organic solvent molecules lead to completely similar bulk behaviors and interfacial properties to those of asphaltenes.

2.1 Simulations. ***Simulated Systems.*** Two types of systems were simulated to probe the effects of temperature and salinity on the IFTs: 1) water/toluene interfaces in the absence of VO-79, and 2) water/toluene interfaces in the presence of VO-79. In total, 8 systems were constructed, and their details are given in Table 1.

The first 4 systems in Table 1 involve water/toluene interfaces in the absence of VO-79 molecules. To construct the initial configurations for these 4 systems, a box of dimensions $6 \times 6 \times 3$ nm^3 was first filled with water molecules. Then the water box was expanded in the z direction for an additional length of 3 nm. The rest of the box was filled with toluene molecules, generating the water/toluene interface in the xy plane (systems WT and WT-350K). Following this, in order to study the salinity effect, a certain number of water molecules were replaced by Na^+ and Cl^- ions to achieve the salt concentration of, respectively, 15 wt% (system WT-S-15%)

and 28 wt% (system WT-S-28%) in aqueous phase. The added Na^+ and Cl^- ions are of equal amount to keep the simulated systems electronically neutral.

The next 4 systems in Table 1 were constructed to probe the effects of temperature and salinity in the presence of VO-79 molecules. The initial configurations for these 4 systems were adopted from our previous work (system 180-T in Ref[35]), and used without modification for the systems VO-WT and VO-WT-350K. For the systems VO-WT-S-15% and VO-WT-S-28%, an appropriate number of water molecules was replaced by Na^+ and Cl^- ions. It is of great importance to point out here that the 180 asphaltene molecules (corresponding to an extremely high bulk concentration ~150000 ppm) employed in these 4 systems are necessary in order to achieve surface concentration of VO-79 similar to that in experiments, below which no apparent reduction of the toluene/water IFT was caused by VO-79.[35]

Simulation Details. The topologies for VO-79 and toluene molecules was built in our previous work[27,35] based on GROMOS96 force field parameter set 53A6,[43] and were directly applied here. For the aqueous phase, a simple-point-charge (SPC) model[44] was used for water, which has been extensively tested for interfacial studies.[32,45,46] As for the ions, their parameters are available in the default GROMOS96 53A6 force field.[43]

All systems were simulated using GROMACS (version 4.6.5).[47-50] For each system, we first performed static structure optimization to ensure the maximum force is less than 1000.0 kJ/(mol*nm). Full dynamics simulations were conducted in NP_nAT ensemble for 10 ns, where P_n and A are, respectively, the normal pressure perpendicular to the interface and the interfacial area in the xy plane. During all the full dynamics simulations, the time step was 2 fs; van der Waals interaction was treated using a twin-range cut-off scheme; long-range electrostatic interaction was handled using particle-mesh Ewald method;[51] average normal pressure was kept at 1 bar using Parrinello – Rahman barostat;[52] temperature was maintained at 350 K for systems WT-350K and VO-WT-350K, and at 300 K for all other systems using a velocity rescaling thermostat[53]. It should be mentioned that this newly developed thermostat is based on correctly reproducing the distribution of kinetic energy under constant temperature, and thus is an accurate method.[53]

The applicability of NP_nAT ensemble for investigating the IFT of organic solvent/water interfaces, as well as the procedure to calculate IFT, was described and validated in our previous work.[35] Appropriate postprocessing tools in GROMACS were used for analysis, and VMD[54] used for visualization.

2.2 Experiments. To validate the IFT trends observed in our theoretical studies, we performed experiments to measure the IFTs of VO-79 toluene solution/water binary systems. Several methods exist to measure IFT, including the recently developed survismeter by Singh[55], which can simultaneously measure surface tension and viscosity of liquids. In this work, IFTs were measured using the pendant drop method with a standard goniometer/tensiometer (ramé-hart, USA). To probe the effects of temperature and salinity, two types of solutions, one of 1000 ppm and the other of 5000 ppm VO-79 in toluene, were first prepared. Then in the case of former, the IFT was measured at 293 K and 323 K maintained by a ramé-hart proportional temperature controller and an environmental chamber, which allows precise temperature regulation between

293 K and 573 K. In the latter case, the aqueous phase was replaced by a solution of 15wt% NaCl in water. In these studies, solvent (i.e. toluene) and salt (i.e. NaCl) were purchased from Sigma-Aldrich; the VO-79 compound was obtained from Alfa Aesar. All reagents were analytical graded and used as received without further modification.

In all our measurements, the tensiometer was set on a vibration-resistant table, which minimizes the droplet deformation due to vibrational shocks. In addition, the measurements were performed in a closed chamber to avoid air fluctuation. The temperature was also constantly checked by means of an external thermometer and no significant fluctuation was observed. Other details on experimental setup and data analysis can be found elsewhere.[35]

3. RESULTS AND DISCUSSION

Figure 2 shows the experimental and simulated IFT values obtained in this work. Quantitatively, since different temperatures, as well as different VO-79 concentrations, were employed, there is a difference between the IFT values from our experiments and those from MD simulations. However, the IFTs obtained share similar trends, confirming our theoretical methodology and findings. Therefore, to understand the mechanisms of the temperature and salinity effects on the IFTs, below, we presented a detailed analysis of our simulated systems.

3.1. Temperature Effect. From Figure 2a, regardless of the presence of VO-79, increasing temperature brings forth a reduction on the IFT of water/toluene interface, consistent with the reported temperature effect in the literature.[6-12] It has long been validated that compared to apolar organic solvents, the high surface tension of water, and hence its high IFT with organic solvent, results from the hydrogen bonding networks in water.[56,57] That is, due to the strong cohesive forces among water molecules, it requires a large amount of work to create a unit area of free water surface (see the energy definition of IFT in Ref[56, 57]). Therefore, we calculated the number of hydrogen bonds formed among water molecules at different temperatures and then normalized them with respect to the number of water molecules. After normalization, these data were plotted in Figure 3a for systems WT and WT-350K. Clearly, increasing temperature decreases the average number of hydrogen bonds per water molecule, consistent with the literature findings.[58,59] At an elevated temperature, with fewer hydrogen bonds formed, the energy required to create a unit area of free water surface is reduced, thus leading to a decreased IFT.

The disruption of hydrogen bonds among water molecules may help with increasing the miscibility of toluene and water phases, thus leading to more reduction of the IFTs. To probe this mechanism, in Figure 3b, we plotted the cumulative number (CN) of toluene atoms around the center of mass (COM) of water phase for systems WT and WT-350K (for details of this calculation, see Supporting Information, section S1). These CNs were normalized with respect to the total number of toluene molecules in each system. Therefore, they can have a very small absolute value. As can be seen, within a short distance ($\leq$ 1 nm), the blue line, which represents the system simulated at 300 K, is 0 till 0.76 nm, whereas the black line (350K) becomes nonzero at ~0.22 nm and is above the blue line (300K) up to ~1.08 nm. This suggests that at 350 K, more toluene atoms can be found in the vicinity of the water COM. In fact, it was observed that during the 10 ns simulation, one toluene molecule entered the bulk water phase in system WT-350K. That is, at an elevated temperature, toluene and water are slightly more miscible. Our findings confirm, from atomic level, the experimental postulations of Donahue et al.[60] that the IFT of a system is directly correlated with its degree of miscibility.

Furthermore, the decreased number of hydrogen bonds within water molecules represents the reduced cohesive forces in water phase; while the increased miscibility of water and toluene phases corresponds to enhanced adhesive forces between these two phases. This is, the cohesive forces in water are transformed to adhesive forces between water and toluene at an elevated temperature, which results in reductions of the water/toluene IFT. The conclusion here is consistent with the study on "friccohesity" of liquid mixtures by Singh et al.[61,62] According to their work, the increase of forces between dissimilar molecules, at the cost of reducing cohesive forces between similar molecules, can lead to a decreased IFT.

As shown in Figure 2a, with the presence of VO-79, similar IFT trend was observed when the temperature is being raised. Therefore, it is expected that compared to the case without VO-79, increasing temperature will affect the number of hydrogen bonds and the miscibility of water and toluene in a similar way. Indeed, the number of hydrogen bonds per water molecule among water (Figure 3c) and the CN of toluene atoms around COM of the water phase (Figure 3d) share similar characteristics, respectively, to those in Figures 3a and 3b. Detailed examination of Figure 3 shows that since Figures 3a and 3c present the normalized number of hydrogen bonds among water molecules (~50,000), the small number of VO-79 molecules did not cause noticeable changes in the number of hydrogen bonds per water molecule. However significant quantitative differences are observed by comparing Figure 3b (in the absence of VO-79) and Figure 3d (in the presence of VO-79). Firstly, the CN curves in Figure 3d become nonzero at a large toluene atom – water COM distance. This is caused by the larger system size (see Table 1) with the presence of VO-79, as well as by sandwiching VO-79 between the two phases. Secondly, it can be seen that the difference between the two curves in Figure 3d is greater than that in Figure 3b. That is, with the presence of VO-79, the number of toluene atoms in the vicinity of the water phase COM is more evidently increased at an elevated temperature (350 K) than its counterpart in the absence of VO-79. Therefore it seems to suggest that the enhancement, in the miscibility of toluene and water molecules, by higher temperature is more significant with the presence of VO-79 molecules. Intuitively, one may expect this greater enhancement in miscibility to cause larger reduction of the IFT with increasing temperature in the systems containing VO-79 molecules. However, from Figure 2a, the reduction of the IFT from 300 K to 350 K is 1.7 mN/m (5.40%) with the presence of VO-79, smaller than the corresponding value, 3.9 mN/m (11.0%), in the absence of VO-79. To understand these apparent discrepancies, it is necessary to further analyze the systems involving VO-79 molecules.

Figure 4 shows the density profile for the systems VO-WT and VO-WT-350K. The density profiles plotted here were computed along the *z* direction, i.e. the direction perpendicular to the interface. Clearly, VO-79 molecules accumulate near the interface at both temperatures. However, at a higher temperature (350 K), the accumulation is less evident, reflected by a smaller peak in the dashed blue line. Furthermore, as shown inset in Figure 4, at an elevated temperature (350 K), the density curve of VO-79 shows a non-zero value in the toluene phase, suggesting that at 350 K, a small amount of VO-79 molecules migrates to the bulk toluene phase. This is, the adsorption of VO-79 molecules is more reversible in toluene with increasing temperature. In our previous work,[35] it has been demonstrated that the accumulation of VO-79 molecules near the interface reduced the IFT of water/toluene interface. Therefore, the slight migration of VO-79 molecules from the interface to the bulk toluene phase at 350 K, can decrease the adhesive forces on the interface, and thus bring in adverse effects to the IFT reduction, which is opposite to the decrement effect of temperature. Hence the reduction in IFT is less significant with the presence of VO-79.

3.2. Salinity Effect. In contrast to the temperature effect (Figure 2a), Figure 2b indicates that the addition of inorganic salts results in an increment of IFTs, regardless of whether VO-79 is present or not. Indeed, this finding is in line with and similar to that observed for the IFTs of water/organic-solvents in the literature.[6-11] To understand the effect of salt ions observed here, we first plotted, in Figure 5, the density profiles for the systems involving sodium chloride salt. As a comparison, the density profiles of the two reference systems (WT and VO-WT) were also plotted. Again, the density was computed along the direction perpendicular to the interface (i.e. the z direction).

Let's first consider Figure 5a. As can be seen, the sodium and chloride ions are mainly distributed in the bulk water phase. Hence we can choose the Gibbs dividing plane to be located at the intersection of water/toluene density curves (see Figure S2 in the Supporting Information for a schematic representation). Then the surface excess of salt is[63]:

$$\Gamma = \frac{M_{ion} - \rho_{bulk1} V_{water} - \rho_{bulk2} V_{toluene}}{A} \quad (1)$$

where Γ is the surface excess (kg/m^2), M_{ion} is the total mass of ions, Na^+ or Cl^-, (kg), and A is the interfacial area (m^2). Furthermore, V_{water} and $V_{toluene}$ are, respectively, the volume (m^3) of water and toluene phases; ρ_{bulk1} and ρ_{bulk2} are the concentrations of ions (kg/m^3), respectively, in the bulk water phase and in the bulk toluene phase (for details on how the bulk water phase and bulk toluene phase are determined, see Supporting Information, Section S2). Since ρ_{bulk1} is the averaged density of ions in the bulk water phase where majority of the ions accumulate, $\rho_{bulk1} > \frac{M_{ion}}{V_{water}}$ (see Supporting Information, Section S2). For ρ_{bulk2} , because there is no ions in the bulk toluene phase, $\rho_{bulk2} = 0$. Thus, it is clear from Eq. (1), that each type of ions has a negative surface excess at the water/toluene interface. According to the Gibbs adsorption isotherm[64]:

$$\Gamma = -\frac{M_m}{RT}\frac{d\gamma}{dlnc} \quad (2)$$

a negative surface excess results in a net increase in the IFT as increasing the bulk concentrations of ions. Here, Γ is the surface excess (kg/m^2), M_m is the molar mass of ions, c is the bulk concentration of ions (mol/L), R is the universal gas constant ($J/(K \times mol)$), T is temperature (K), and γ is the IFT (N/m). From physics point of view, Na^+ and Cl^- ions are hydrated in water, and can realign water molecules to form ion-dipole interactions with water.[65] Therefore these hydrated ions can increase the cohesive forces between the water molecules, and thus increase the energy needed to create a unit area of free water surface, leading to an increased IFT.[66]

As mentioned before, in the presence of VO-79 molecules, adding salts also leads to an increased IFT (Figure 2b). Therefore, it is expected that the above discussion should be applicable to systems involving VO-79 molecules. However, detailed examination of Figure 2b reveals that unlike the significant IFT change in systems without VO-79, the IFT in system VO-WT-S-15% is nearly identical to that in system VO-WT. Even with 28 wt% of salts, in the presence of VO-79, the increment effect of salts on the IFT (1.8 mN/m, 5.71%) is less evident than that in the absence of VO-79 (5.6 mN/m, 15.9%). These observations suggest that with the presence of VO-79, the effect of ions on the IFT is again lightened. To understand this phenomenon, it is necessary to examine the density profiles for systems having VO-79; these were plotted in Figure 5b (system VO-WT-S-15% is omitted here due to its insignificant change in the IFT compared to system VO-WT as discussed above).

It can be seen, from Figure 5b, that ions are mainly distributed in the water phase, similar to that in the absence of VO-79 molecules. Therefore, Na^+ and Cl^- generate negative surface excess at the interface, thus leading to the IFT increment in system VO-WT-28%. Further inspection of Figure 5b shows that the curve for the distribution of VO-79 in system VO-WT-S-28% has a much sharper peak at the interface than that in system VO-WT, indicating that the accumulation of VO-79 at the interface is more prominent with the addition of salt. The stronger accumulation of VO-79 can cause an increase in the adhesive forces at the interface, which tends to decrease the IFT and thus brings in adverse effect in comparison with the effect of salt alone.

The stronger accumulation of VO-79 molecules at the interface, introduced by the addition of salt, might be attributed to the enhanced electrostatic forces between VO-79 and the water phase. While our VO-79 molecules are electrostatically neutral, their oxygen moieties are polar functional groups. Therefore, it is expected that these polar functional groups can possess electrostatic interactions with ions. That is, despite that majority of the ions are in the bulk, a small fraction of ions is still in contact with VO-79. Indeed, as shown in Figure 5b, the curves representing the distribution of ions intersect with that of VO-79, indicating the overlapping occurrence of ions and VO-79 at the interface. The electrostatic attractions between ions and VO-79 can be further verified by the slightly decreased aggregation extent of VO-79 in system

VO-WT-S-28%. Figure 6 shows the radial distribution function (RDF) for the center of geometry (COG) separation between polyaromatic cores of VO-79 molecules. It can be clearly seen that the first peak of the RDF is slightly decreased in system VO-WT-S-28% compared to that in system VO-WT. As the sharpness of the first peak in the RDF is an indicator of the interaction strength between two parallel stacked polyaromatic cores,[26, 27] the results here confirm that the presence of ions in the aqueous phase can also slightly modulate the interactions in the toluene phase, leading to the stronger accumulation of VO-79 near the interface. Interestingly, the slightly decreased aggregation extent of VO-79, induced by the addition of ions, shares certain similarities with the "salting-in" effect of ions on increasing the solubility of proteins in water.[67]

It is of great importance to emphasize here that the particular IFT trend observed in this work depends on the solvent property and the specific structure of model asphaltene compounds as well as the ion species (monovalent salts vs. divalent salts). For instance, our model asphaltene compounds cannot be ionized, thus leading to that insignificant amount of salt ions can migrate to the interface. Contrarily, in the work of Moeini et al.,[12] asphaltenes were proposed to have different degrees of ionization with increasing salt concentrations. That is, the presence of asphaltenes greatly affected the salt ion distribution with respect to the interface, resulting in a non-monotonic relation between the IFT of an Iranian crude oil/brine water interface and the salt concentration. [12]

3.3. IFT reduction of toluene/water interface due to the presence of VO-79. From the above discussion, it is clear that the presence of VO-79 can alleviate the effect of temperature and salt on the IFT of water/toluene interface. This effect is resulted from the fact that the accumulation of VO-79 near the interface can decrease the IFT of toluene/water interface from that in the absence of VO-79, and contrarily, the migration of VO-79 from the interface to the bulk tends to increase the IFT. In our previous work,[35] it was reported that the hydrogen bonds formed between Oxygen atoms on VO-79 and water molecules can drive the reduction of water/toluene IFT. This is, these hydrogen bonds can be one major component of the adhesive forces between VO-79 solution and water phase. Therefore, in this section, we further probe the correlation between the effect of VO-79 on the IFT of toluene/water interface and the number of hydrogen bonds formed between VO-79 and water molecules. These data are shown in Figure 7, where $\Delta\gamma = \gamma_a - \gamma_p$ with γ_a and γ_p, respectively, being the IFT of water/toluene interface in the absence and presence of VO-79 molecules, and n represents the number of hydrogen bonds formed between VO-79 and water molecules.

As can be seen from Figure 7, clearly, the reduction effect of VO-79 on the IFT ($\Delta\gamma$) is well correlated with the number of hydrogen bonds formed between VO-79 and water molecules (n), i.e. a larger number of hydrogen bonds result in a more significant reduction in the IFT. Specifically, with the addition of salts, as VO-79 molecules further concentrate near the interface (see section 3.2), more hydrogen bonds are formed, leading to a larger reduction in the IFT (point marked by (300 K, 28% salt) in Figure 7). In contrast, with elevating temperature, VO-79 molecules become more toluene-soluble and can migrate to the bulk toluene phase (see section 3.1). Therefore, VO-79 molecules are less concentrated near the interface, resulting in that fewer hydrogen bonds are formed between VO-79 and water molecules. The less hydrogen bonding then leads to a small reduction in the IFT (point marked by (350 K, 0% salt) in Figure 7). These observations clearly demonstrate, again, that hydrogen bonding between VO-79 and water molecules is one of the adhesive forces driving the IFT reduction.

4. CONCLUSIONS

In this work, we have clarified the underlying mechanisms for the effect of temperature and salinity on the IFTs of toluene/water interface. It was first demonstrated that in the absence of model asphaltene compounds (VO-79), elevating temperature decreases the number of hydrogen bonds formed among water molecules. Therefore, the energy required to create a unit area of free water is reduced, leading to a decreased IFT. Moreover, at higher temperatures, the miscibility of water and toluene is increased, which helps to further reduce the IFT. Contrarily, the addition of monovalent salts (NaCl) into aqueous phase increases the IFTs of water/toluene interface. This can be attributed to the hydration of ions, which result in a negative surface excess of ions at the interface and thus increase the free energy needed for creating a unit area of free water surface. Compared to the cases without model asphaltenes, similar observations were obtained for the effects of temperature and salinity in the presence of VO-79 molecules. However, the extent of those effects was evidently alleviated, which resulted from the fact that the distribution of VO-79 molecules, with respect to the water/toluene interface, can be affected by the temperature variation and the presence of salt. The results reported here provide fundamental insights into how the IFTs can be modulated by temperature and salt, and thus can help to control the IFTs in petroleum processing.

Acknowledgement

We acknowledge the computing resources and technical support from Western Canada Research Grid (WestGrid). Financial support from the Natural Science and Engineering Research Council (NSERC) of Canada, Canadian Centre for Clean Coal/Carbon and Mineral Processing Technologies (C^5MPT), Alberta Innovates – Energy and Environment Solutions (AI-EES) and Nexen Energy ULC is gratefully acknowledged.

Supporting Information

Schematic representation of toluene distribution around the center of mass (COM) of the water phase, illustration on the Gibbs dividing plane and bulk solvent phases for calculating the surface excess of ions.

References

1. Anastasiadis, S. H.; Gancarz, I.; Koberstein, J. T. *Macromolecules* **1988***, 21,* 2980-2987.

2. Hu, W.; Koberstein, J. T.; Lingelser, J.; Gallot, Y. *Macromolecules* **1995***, 28,* 5209-5214.

3. Mayoral, E.; Goicochea, A. G. *J. Chem. Phys.* **2013***, 138,* 094703.

4. Taber, J. *Society of Petroleum Engineers Journal* **1969***, 9,* 3-12.

5. Morrow, N.; Buckley, J. *J. Pet. Technol.* **2011***, 63,* 106-112.

6. Wiegand, G.; Franck, E. *Ber. Bunsenges./Phys. Chem. Chem. Phys.* **1994***, 98,* 809-817.

7. Zeppieri, S.; Rodríguez, J.; López de Ramos, A. *J. Chem. Eng. Data* **2001***, 46,* 1086-1088.

8. Al-Sahhaf, T.; Elkamel, A.; Suttar Ahmed, A.; Khan, A. *Chem. Eng. Commun.* **2005***, 192,* 667-684.

9. Jennings, H. Y. *J. Colloid Interface Sci.* **1967***, 24,* 323-329.

10. Cai, B.; Yang, J.; Guo, T. *J. Chem. Eng. Data* **1996***, 41,* 493-496.

11. Ikeda, N.; Aratono, M.; Motomura, K. *J. Colloid Interface Sci.* **1992***, 149,* 208-215.

12. Moeini, F.; Hemmati-Sarapardeh, A.; Ghazanfari, M.; Masihi, M.; Ayatollahi, S. *Fluid Phase Equilib.* **2014***, 375,* 191-200.

13. Lashkarbolooki, M.; Ayatollahi, S.; Riazi, M. *J. Chem. Eng. Data* **2014***, 59,* 3624-3634.

14. Poteau, S.; Argillier, J.; Langevin, D.; Pincet, F.; Perez, E. *Energy Fuels* **2005***, 19,* 1337-1341.

15. Rane, J. P.; Harbottle, D.; Pauchard, V.; Couzis, A.; Banerjee, S. *Langmuir* **2012***, 28,* 9986-9995.

16. Rane, J. P.; Pauchard, V.; Couzis, A.; Banerjee, S. *Langmuir* **2013***, 29,* 4750-4759.

17. Pauchard, V.; Rane, J. P.; Banerjee, S. *Langmuir* **2014***, 30,* 12795-12803.

18. Lashkarbolooki, M.; Riazi, M.; Ayatollahi, S.; Hezave, A. Z. *Fuel* **2016***, 165,* 75-85.

19. Guo, J.; Liu, Q.; Li, M.; Wu, Z.; Christy, A. A. *Colloids Surf. Physicochem. Eng. Aspects* **2006***, 273,* 213-218.

20. Gao, S.; Moran, K.; Xu, Z.; Masliyah, J. *J. Phys. Chem. B* **2010***, 114,* 7710-7718.

21. Headen, T. F.; Boek, E. S.; Skipper, N. T. *Energy Fuels* **2009***, 23,* 1220-1229.

22. Teklebrhan, R. B.; Ge, L.; Bhattacharjee, S.; Xu, Z.; Sjöblom, J. *J. Phys. Chem. B* **2012***, 116,* 5907-5918.

23. Sedghi, M.; Goual, L.; Welch, W.; Kubelka, J. *J. Phys. Chem. B* **2013***, 117,* 5765-5776.

24. Frigerio, F.; Molinari, D. *Comp. Theor. Chem.* **2011***, 975,* 76-82.

25. Kuznicki, T.; Masliyah, J. H.; Bhattacharjee, S. *Energy Fuels* **2008***, 22,* 2379-2389.

26. Jian, C.; Tang, T.; Bhattacharjee, S. *Energy Fuels* **2013**, *27*, 2057 − 2067.

27. Jian, C.; Tang, T.; Bhattacharjee, S. *Energy Fuels* **2014,** *28,* 3604-3613.

28. Jian, C.; Tang, T. *The Journal of Physical Chemistry B* **2014**.

29. Jian, C.; Tang, T. *J. Phys. Chem. B* **2015***, 119,* 8660-8668.

30. Gao, F.; Xu, Z.; Liu, G.; Yuan, S. *Energy Fuels* **2014***, 28,* 7368-7376.

31. Teklebrhan, R. B.; Ge, L.; Bhattacharjee, S.; Xu, Z.; Sjöblom, J. *J. Phys. Chem. B* **2014**, *118,* 1040 − 1051.

32. Kuznicki, T.; Masliyah, J. H.; Bhattacharjee, S. *Energy Fuels* **2009***, 23,* 5027-5035.

33. Ruiz-Morales, Y.; Mullins, O. C. *Energy Fuels* **2015***, 29,* 1597-1609.

34. Liu, J.; Zhao, Y.; Ren, S. *Energy Fuels* **2015**, *29,* 1233-1242.

35. Jian, C.; Poopari, M. R.; Liu, Q.; Zerpa, N.; Zeng, H.; Tang, T. *J. Phys. Chem. B* **2016**, *120,* 5646-5654.

36. Park, J.; Moon, J. *Langmuir* **2006**, *22,* 3506-3513.

37. Chen, S.; Slattum, P.; Wang, C.; Zang, L. *Chem. Rev.* **2015**, *115,* 11967-11998.

38. Weinstein, S. J.; Ruschak, K. J. *Annu. Rev. Fluid Mech.* **2004**, *36,* 29-53.

39. Sztukowski, D. M.; Yarranton, H. W. *Langmuir* **2005**, *21,* 11651-11658.

40. Wang, S.; Liu, J.; Zhang, L.; Xu, Z.; Masliyah, J. *Energy Fuels* **2008**, *23,* 862-869.

41. Schuler, B.; Meyer, G.; Peña, D.; Mullins, O. C.; Gross, L. *J. Am. Chem. Soc.* **2015**, *137,* 9870-9876.

42. Yang, F.; Tchoukov, P.; Dettman, H.; Teklebrhan, R. B.; Liu, L.; Dabros, T.; Czarnecki, J.; Masliyah, J.; Xu, Z. *Energy Fuels* **2015**, *29,* 4783-4794.

43. Oostenbrink, C.; Villa, A.; Mark, A. E.; Van Gunsteren, W. F. *J. Comput. Chem.* **2004**, *25,* 1656-1676.

44. Berendsen, H. J. C.; Postma, J. P. M.; van Gunsteren, W.; Hermans, J. Interaction Models for Water in Relation to Protein Hydration. In *In Intermolecular Forces;* Pullmann, B., Ed., Ed.; D. Reidel Publishing Company: Dordrecht, The Netherlands, 1981; pp 331 −342.

342. 45. Tieleman, D.; Berendsen, H. *J. Chem. Phys.* **1996**, *105,* 4871-4880.

46. Zielkiewicz, J. *J. Chem. Phys.* **2005***, 123,* 104501.

47. Hess, B.; Kutzner, C.; Van Der Spoel, D.; Lindahl, E. *J. Chem. Theory Comput.* **2008***, 4,* 435-447.

48. Van Der Spoel, D.; Lindahl, E.; Hess, B.; Groenhof, G.; Mark, A. E.; Berendsen, H. J. C. *J. Comput. Chem.* **2005***, 26,* 1701-1718.

49. Lindahl, E.; Hess, B.; van der Spoel, D. *J. Mol. Model.* **2001***, 7,* 306-317.

50. Berendsen, H. J. C.; van der Spoel, D.; van Drunen, R. *Comput. Phys. Commun.* **1995***, 91,* 43-56.

51. Essmann, U.; Perera, L.; Berkowitz, M. L.; Darden, T.; Lee, H.; Pedersen, L. G. *J. Chem. Phys.* **1995***, 103,* 8577.

52. Parrinello, M.; Rahman, A. *J. Appl. Phys.* **1981***, 52,* 7182-7190.

53. Bussi, G.; Donadio, D.; Parrinello, M. *J. Chem. Phys.* **2007***, 126,* 014101.

54. Humphrey, W.; Dalke, A.; Schulten, K. *J. Mol. Graphics* **1996***, 14,* 33-38.

55. Singh, M. *J. Biochem. Biophys. Methods* **2006***, 67,* 151-161.

56. Barnes, G.; Gentle, I. *Interfacial Science: An Introduction;* Oxford University Press: Oxford, U. K. **2005**.

57. Israelachvili, J. N. *Intermolecular and Surface Forces,* 3rd ed.; Academic press: London, **2011**.

58. Jorgensen, W. L.; Madura, J. D. *Mol. Phys.* **1985**, *56,* 1381-1392.

59. Mizan, T. I.; Savage, P. E.; Ziff, R. M. *J. Phys. Chem.* **1996**, *100,* 403-408.

60. Donahue, D. J.; Bartell, F. *J. Phys. Chem.* **1952**, *56,* 480-484.

61. Chandra, A.; Patidar, V.; Singh, M.; Kale, R. *J. Chem. Thermodyn.* **2013**, *65,* 18-28.

62. Singh, M. *J. Mol. Liq.* **2014**, *200,* 289-297.

63. Graf, K.; Kappl, M. *Physics and chemistry of interfaces;* Wiley-VCH: Weinheim, Germany, **2006**.

64. Rosen, M. J.; Kunjappu, J. T. *Surfactants and interfacial phenomena,* 4th ed.; John Wiley & Son: Hoboken, NJ, **2012**.

65. Mancinelli, R.; Botti, A.; Bruni, F.; Ricci, M.; Soper, A. *J. Phys. Chem. B* **2007**, *111,* 13570-13577.

66. Weissenborn, P. K.; Pugh, R. J. *Langmuir* **1995**, *11,* 1422-1426.

67. Arakawa, T.; Timasheff, S. N. *Biochemistry* **1984**, *23,* 5912-5923.

Figures

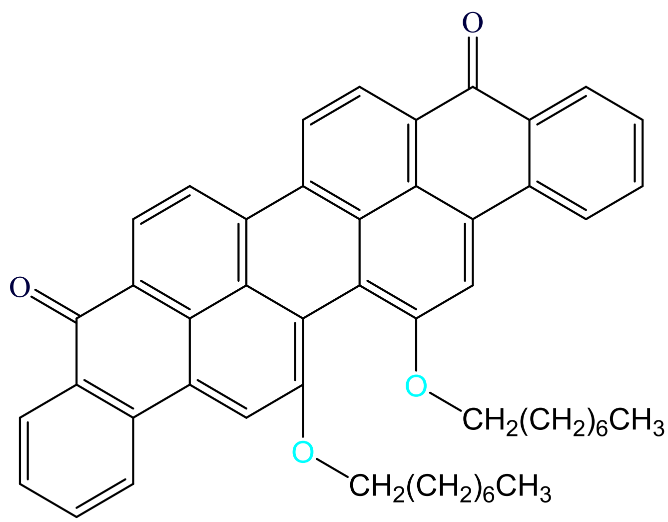

Figure 1. Chemical structure of the molecular model employed in this work.

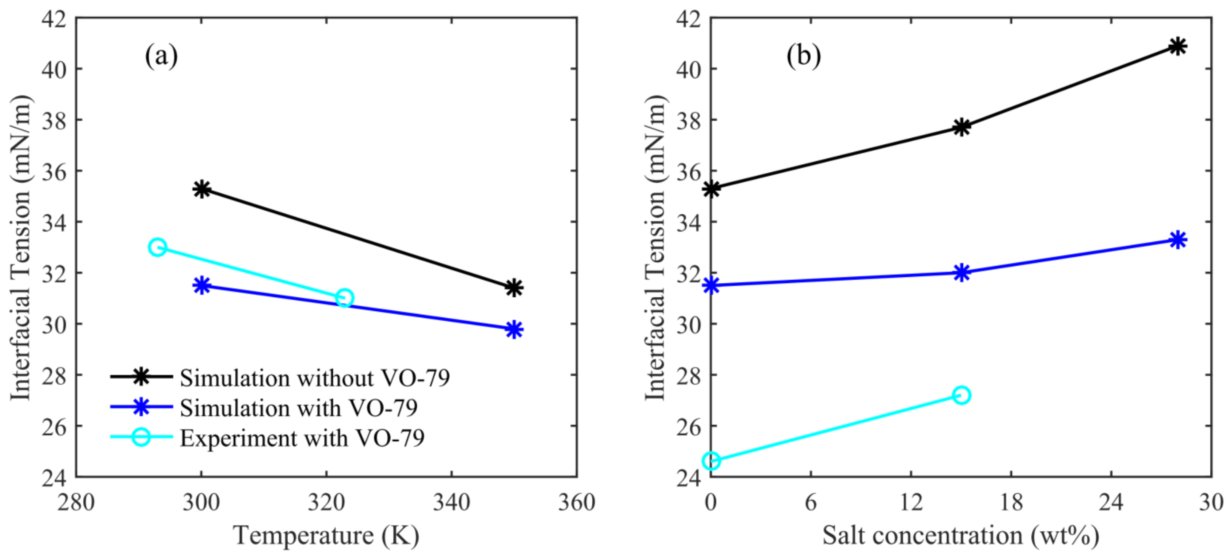

Figure 2. IFT as a function of (a) temperature and (b) salt concentration. Lines are drawn for a guide of eyes.

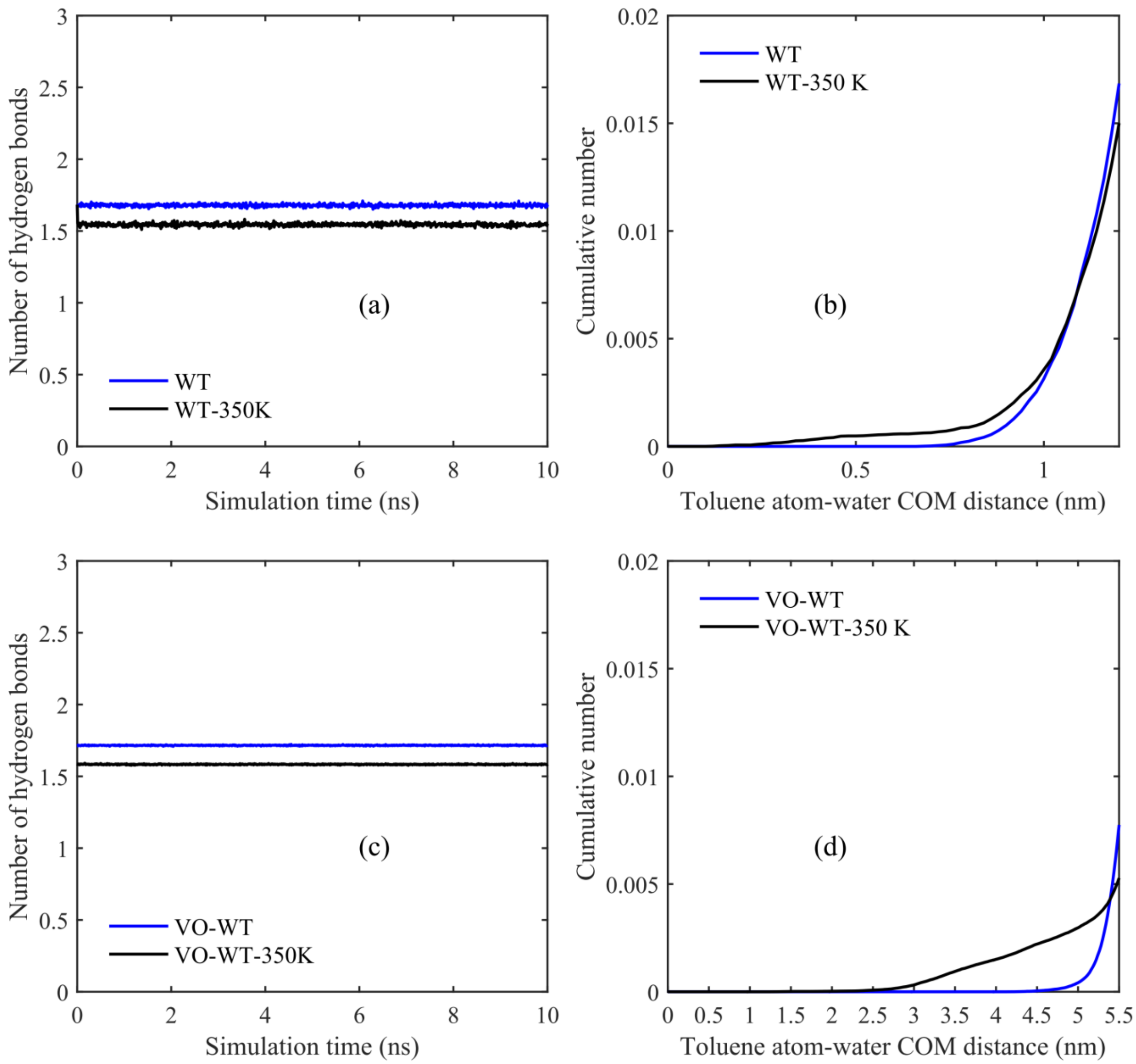

Figure 3. Average number of hydrogen bonds per water molecule in systems (a) WT and WT-350K, and (c) VO-WT and VO-WT-350K; toluene distribution around COM of the water phase in systems (b) WT and WT-350K, and (d) VO-WT and VO-WT-350K.

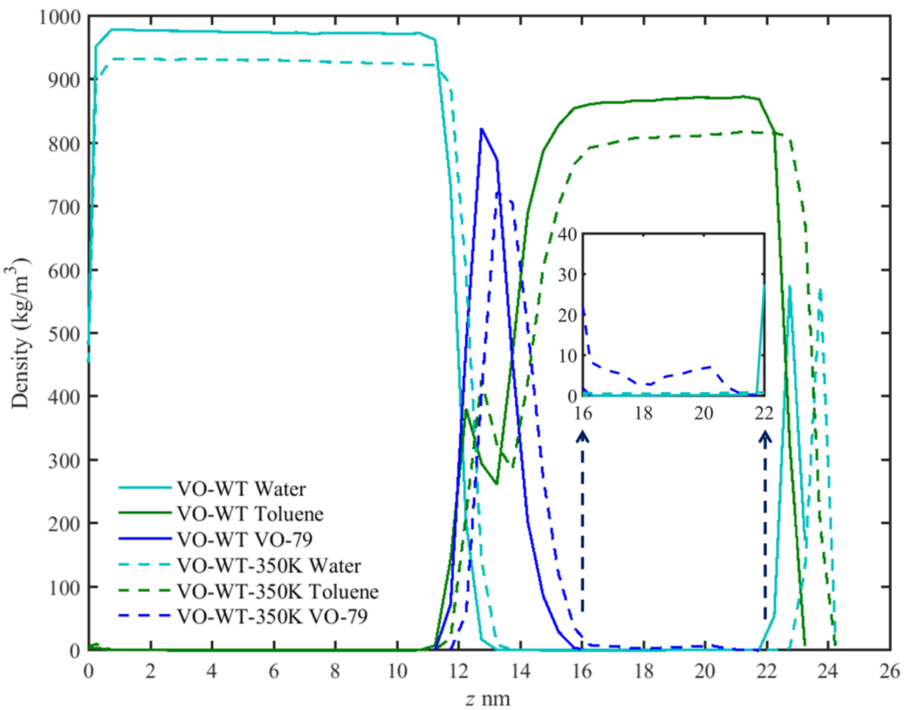

Figure 4. Density profile for systems VO-WT and VO-WT-350K. The water phase is on the left and toluene phase on the right. In the legend, curves from the same system are grouped together, each of which is designated by the system name plus the substance. For instance, VO-WT-350K VO-79 corresponds to the density profile of VO-79 in system VO-WT-350K.

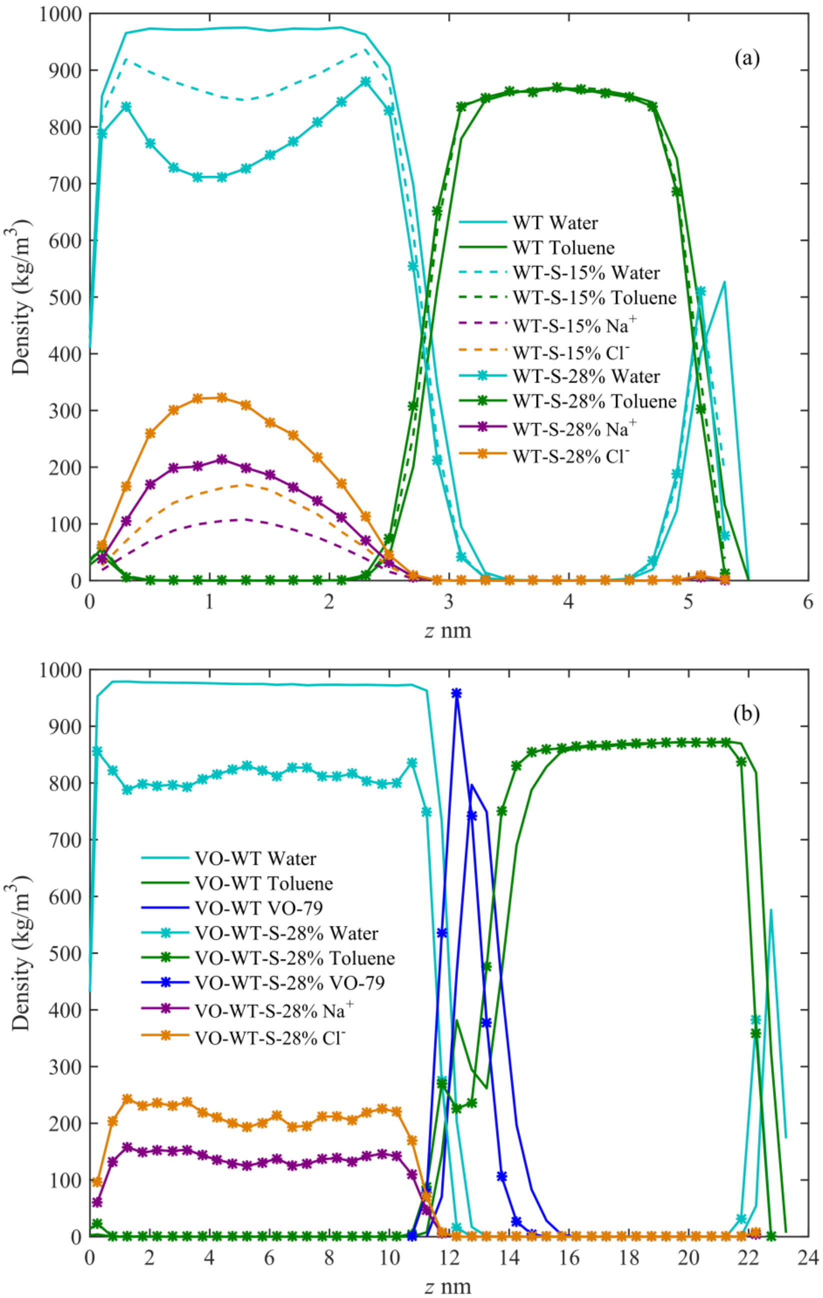

Figure 5. Density profiles for systems (a) WT, WT-S-15%, and WT-S-28%, and (b) VO-WT and VO-WT-S-28%. In the two subfigures, the water phase is on the left and toluene phase on the right. In the legend, curves from the same system are grouped together, each of which is designated by the system name plus the substance. For instance, VO-WT-S-28% VO-79 corresponds to the density profile of VO-79 in system VO-WT-S-28%.

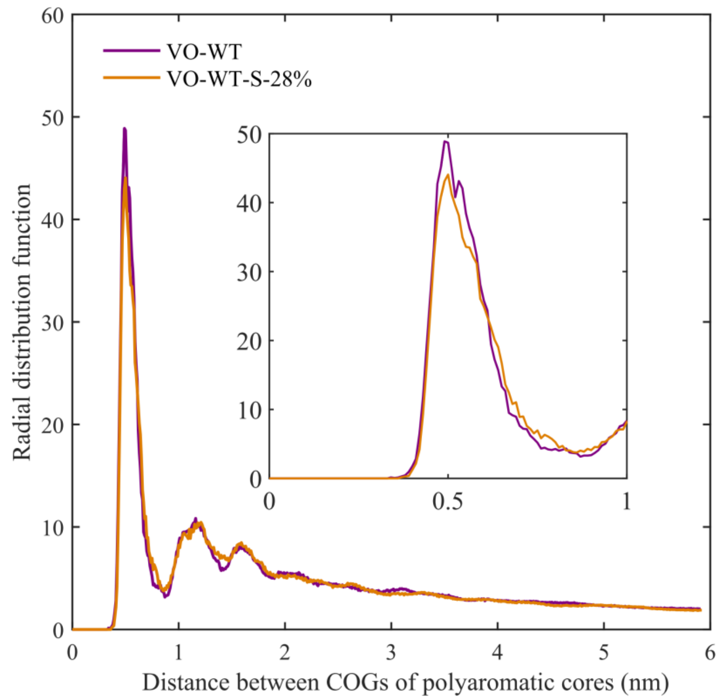

Figure 6. RDF as a function of the distance between COGs of polyaromatic cores (nm).

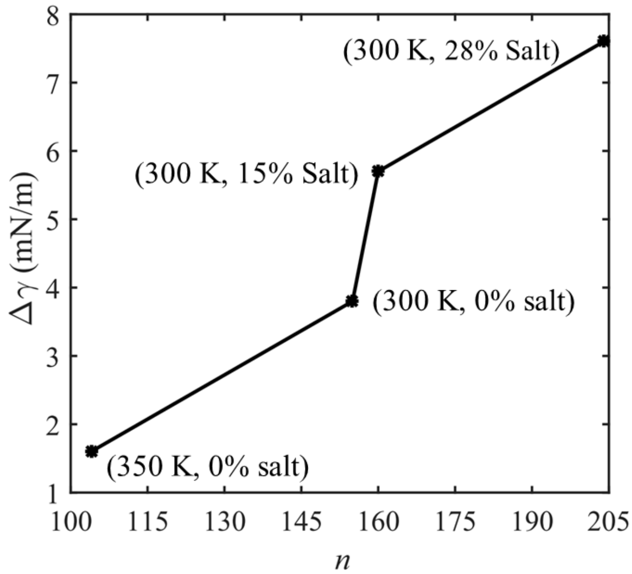

Figure 7. Reduction effect of VO-79 on the IFT ($\Delta\gamma$) as a function of the number of hydrogen bonds formed between VO-79 and water molecules (n). The parentheses denote the conditions for each comparison.

Tables

Table 1. Details of the 8 Systems Simulated

system name	box size (nm^3)	no. of VO-79 molecules	temperature	no. of Na^+/Cl^- ions	salt concentration (wt%)
WT	$6 \times 6 \times 6$	0	300 K	0/0	0
WT-350K	$6 \times 6 \times 6$	0	350 K	0/0	0
WT-S-15%	$6 \times 6 \times 6$	0	300 K	174/174	15%
WT-S-28%	$6 \times 6 \times 6$	0	300 K	348/348	28%
VO-WT	$12 \times 12 \times 24$	180	300 K	0/0	0
VO-WT-350K	$12 \times 12 \times 24$	180	350 K	0/0	0
VO-WT-S-15%	$12 \times 12 \times 24$	180	300 K	2832/2832	15%
VO-WT-S-28%	$12 \times 12 \times 24$	180	300 K	5664/5664	28%